Original Investigation

Heat Generation During Ablation of Porcine Skin With Erbium:YAG Laser vs a Novel Picosecond Infrared Laser

Nathan Jowett, MD, FRCSC; Wolfgang Wöllmer, PhD; Alex M. Mlynarek, MD, MSc, FRCSC; Paul Wiseman, PhD;
Bernard Segal, PhD; Kresimir Franjic, PhD; Peter Krötz, MSc; Arne Böttcher, MD; Rainald Knecht, MD, PhD;
R. J. Dwayne Miller, PhD

IMPORTANCE Despite significant advances in surgery, most surgical tools remain basic. Lasers provide a means of precise surgical ablation, but their clinical use has remained limited because of undesired thermal, ionizing, or acoustic stress effects leading to tissue injury. A novel ultrafast, nonionizing, picosecond infrared laser (PIRL) system has recently been developed and is capable, in theory, of ablation with negligible thermal or acoustic stress effects.

OBJECTIVE To measure and compare heat generation by means of thermography during ablation of ex vivo porcine skin by conventional microsecond-pulsed erbium:YAG (Er:YAG) laser and picosecond infrared laser (PIRL).

DESIGN AND SETTING This study was conducted in an optics laboratory and used a pretest-posttest experimental design comparing 2 methods of laser ablation of tissue with each sample acting as its own control.

INTERVENTION Ex vivo porcine skin was ablated in a 5-mm line pattern with both Er:YAG laser and PIRL at fluence levels marginally above ablation threshold (2 J/cm^2 and 0.6 J/cm^2, respectively).

MAIN OUTCOMES AND MEASURES Peaks and maxima of skin temperature rises were determined using a thermography camera. Means of peak temperature rises were compared using the paired sample t test. Ablation craters were assessed by means of digital microscopy.

RESULTS Mean peak rise in skin surface temperature for the Er:YAG laser and PIRL was 15.0°C and 1.68°C, respectively (P < .001). Maximum peak rise in skin surface temperature was 18.85°C for the Er:YAG laser and 2.05°C for the PIRL. Ablation craters were confirmed on digital microscopy.

CONCLUSIONS AND RELEVANCE Picosecond infrared laser ablation results in negligible heat generation, considerably less than Er:YAG laser ablation, which confirms the potential of this novel technology in minimizing undesirable thermal injury associated with lasers currently in clinical use.

Author Affiliations: Author affiliations are listed at the end of this article.

Corresponding Author: Nathan Jowett, MD, FRCSC, Department of Otolaryngology–Head and Neck Surgery, Jewish General Hospital, 3755 chemin de la Côte-Sainte-Catherine, Ste E-903, Montréal, QC H3T 1E2, Canada (nathan.jowett@mail.mcgill.ca).

D espite significant advances in surgery over the last century, most surgical instrumentation remains basic. It has been well documented that conventional instruments such as scalpels, saws, and drills cause significant tissue trauma through shearing forces, vibrations, and/or thermal injury.[1-3] Furthermore, owing to their inherent imprecision and human operation, use of these crude instruments is not without considerable risk of inadvertent tissue injury. Advances in photonics and laser design have brought great promise for advancing precision in surgical tissue manipulation. Although they offer precision, conventional lasers have since been shown to cause considerable tissue injury through combinations of ionizing, thermal, or acoustic shockwave effects.[2,4,5] As such, their clinical use remains limited.[6]

The introduction of nonionizing, short-pulse microsecond (10^{-6} seconds) and Q-switched nanosecond (10^{-9} seconds) erbium:YAG (Er:YAG) lasers brought hope of achieving a long-desired means of "cold" laser ablation. With shorter pulses, photomechanical ablation is possible, when the absorption of a laser pulse in the target tissue creates mechanical stress leading to material fracture and ejection.[7] Because tissue has a thermal relaxation time on the order of a few microseconds for most types of laser-tissue interactions,[8] the ability to remove it without notable thermal injury using short pulses seemed possible, in theory. However, results from healing studies were disappointing.[2,5,9-11] Because relatively high fluence (defined as the amount of light energy incident on a given square area) levels are required for Er:YAG laser ablation (at >1.5 J/cm²), complete thermal confinement is not possible, and substantial thermal injury due to temperature superposition still occurs.[2,5,11-13] Studies have confirmed thermal necrosis with Er:YAG laser ablation at fluence levels common in clinical practice.[2,5,11] Because irreversible thermal denaturation of human proteins is known to occur at short exposures to temperatures as low as 18°C above body temperature, cellular injury is possible even in the absence of immediately obvious histologic necrosis.[14-17] Furthermore, as a result of acoustic stress relaxation times being on the order of 1 nanosecond for human tissue, even microsecond and Q-switched nanosecond Er:YAG laser pulses result in propagation of acoustic transients that lead to distant fracture of the extracellular matrix, increasing inflammation.[5]

Recently, a new generation of "ultrafast" lasers has been developed.[18] These ultrafast lasers deposit concentrated packets of photons in pulses of picoseconds (10^{-12}) or less, quicker than both the thermal and stress relaxation times of tissue. As such, deleterious thermal and acoustic shockwave effects are negated.[5]

A novel, nonionizing ultrafast picosecond infrared laser (PIRL) system has recently been developed that is capable, in theory, of true "cold" photomechanical ablation.[5] Because this technology is currently in its infancy, data confirming its clinical potential is limited. Previous wound healing studies by Amini-Nik et al[2] have shown zones of injury significantly smaller on scanning electron microscopy for full-thickness incisions made by PIRL compared with scalpel and Er:YAG laser. In addition, the width of the scars formed by PIRL incision were negligible compared with those produced using either Er:YAG laser or scalpel. Furthermore, protein signaling responsible for scar tissue formation was dramatically reduced with PIRL ablation, with no notable scar tissue formation extending away from the ablation margins. This significantly improved healing is presumably due to the very low thermal heating and energy transport to regions beyond the cut zone. To date, no study has directly measured and confirmed negligible tissue heating during active ablation using the PIRL system.

The objective of this study was to measure and compare real-time heat generation during ablation of ex vivo porcine epidermis using a PIRL and conventional microsecond-pulsed Er:YAG laser. It is hypothesized that real-time heat generation, as measured by infrared thermography, will be significantly lower for PIRL ablation than for Er:YAG laser ablation.

Methods

Laser Systems

An Er:YAG laser (MCL 29; Aesculap-Meditec GmbH) and a picosecond infrared laser (PIRL; AttoDyne Inc) were used. The Er:YAG laser and PIRL had pulse lengths of 250 microseconds (250×10^{-6} seconds) and 300 picoseconds (300×10^{-12} seconds), respectively, both with wavelengths of 2.94 μm. For the Er:YAG laser, a 5 × 1-mm slit mode was used. The Er:YAG system uses a scanning process, moving over the area under treatment in an overlapping fashion to ensure uniform ablation. The laser was set to produce 2 passes at a pulse frequency of 24 Hz and pulse energy of 100 mJ, corresponding to a fluence of 2 J/cm² for a 5 × 1-mm slit. This fluence is only slightly higher than the ablation threshold of 1.5 J/cm² for soft tissue for the Er:YAG laser and lower than the typical fluence levels used in clinical applications such as skin resurfacing.[12] For the PIRL, a 5-mm line scan pattern was used. As with the Er:YAG laser, the PIRL system uses a similar scanning process moving over the area under treatment in an overlapping fashion, with the option of selecting the scan speed. The laser was again set to produce a total of 2 passes, with a scan speed of 3 mm/s and a pulse frequency of 50 Hz (the minimum setting for the PIRL system). The PIRL emits a circular Gaussian beam with a diameter of 300 μm. The pulse energy was measured at 0.2 mJ using a digital optical energy meter. Peak Gaussian circular beam fluence (φ_0) is calculated using the following formula:

$$\varphi_0 = \frac{2 \cdot E_p}{\pi r^2}$$

where E_p is the pulse energy and r is the beam radius. With this formula, the corresponding output fluence of the PIRL was calculated to be 0.6 J/cm².

Thermography

Fresh ex vivo porcine full-thickness skin sections, cut into 2.54 × 2.54-cm sections from the dorsal hind leg region of a single specimen, were centered into position on the focal planes of the lasers. The capture field of a thermography camera (PIR uc 180; InfraTec) was then focused onto this same region and

calibrated. Thermography is based on the principle of black-body radiation, whereby any opaque and nonreflective body will emit a characteristic electromagnetic radiation spectrum in a Gaussian curve dependent solely on its temperature. The spectral range of the thermography camera used was 7.5 to 13 μm, selected in order to avoid capturing the thermal signal of the beam itself, which is at a much lower wavelength of 2.94 μm for both lasers. Real-time fast-frame thermal images (at 100 frames per second) were then captured for both systems during pulsed ablation. The peaks in the rises of skin temperature were determined using IRBIS 3plus software (InfraTec). A digital microscope was then used to capture postablation images to confirm the presence of superficial ablation craters within skin sections for both ablation methods.

Figure 1 demonstrates the experimental thermography setup for the PIRL system. The output PIRL beam is shaped,

focused, and combined with a low power helium-neon (red) beam for visibility and controlled with programmable beam-steering mirrors contained within an optics case. The skin sample is placed on the focal plane of the beam on a translation stage. The thermography camera is focused on the skin sample; its output is shown on the laptop screen. A digital microscope is focused on the sample; its output is shown on the desktop screen.

Statistical Analysis

Means of peak temperature recordings were compared using a paired t test with the α level set to .05. For a known standard deviation of 1°C for the thermal images, a modest expected temperature rise of 10°C for the Er:YAG laser ablation, and an α of .05, a single peak temperature measurement per laser would be required to detect a 25% difference in temperature rise between the 2 lasers with a power of 80%. In total, 12 peak temperatures were measured and averaged for the Er:YAG laser in a 2-line pass, with hundreds of measurements recorded and averaged for the PIRL during ablation. Analysis was performed using SPSS 17.0 statistical software (IBM).

Figure 1. Experimental Thermography Setup for the Picosecond Infrared Laser System
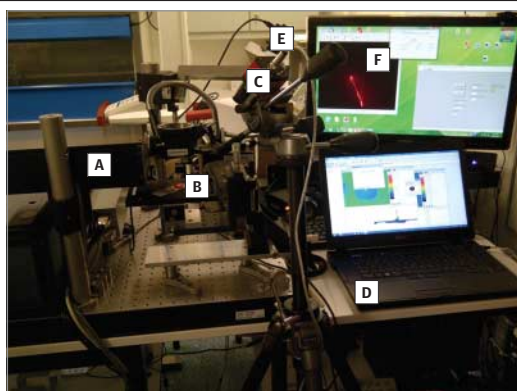

A, Beam shaping optics; B, skin sample on translation stage; C, thermography camera; D, thermography camera output screen; E, digital microscope; F, output screen of digital microscope.

Results

Figure 2 demonstrates representative thermal images captured during ablation for the Er:YAG laser and PIRL. The images are color mapped; the color gradient on the right of each image demonstrates increases in temperatures from black-blue (cold) to violet-white (hot). Only thermal data within the white circular region (of approximately 7 mm diameter) is captured. As is clearly demonstrated, consistently significantly hotter regions are seen on the Er:YAG laser thermal images compared with those generated using the PIRL. It is important to note that the color gradient legend for the Er:YAG laser ablation varies from 29°C (black-blue) to 51°C (violet-white). The

Figure 2. Thermal Image Frames
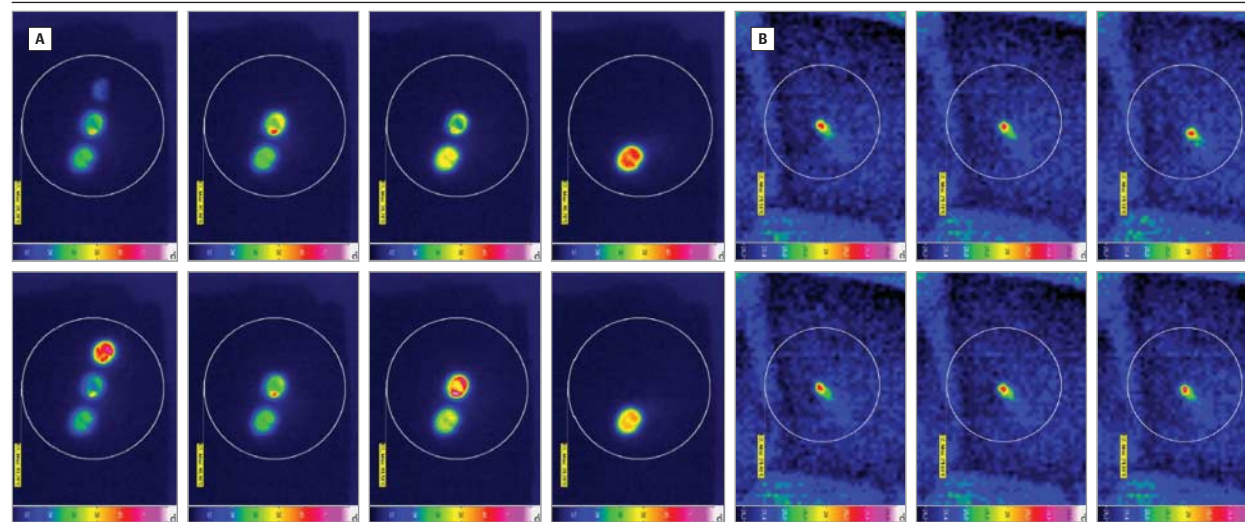
A, Representative thermal image frames from erbium:YAG laser ablation. B, Representative thermal image frames from picosecond infrared laser system ablation.

Figure 3. Thermograms for Laser Ablation
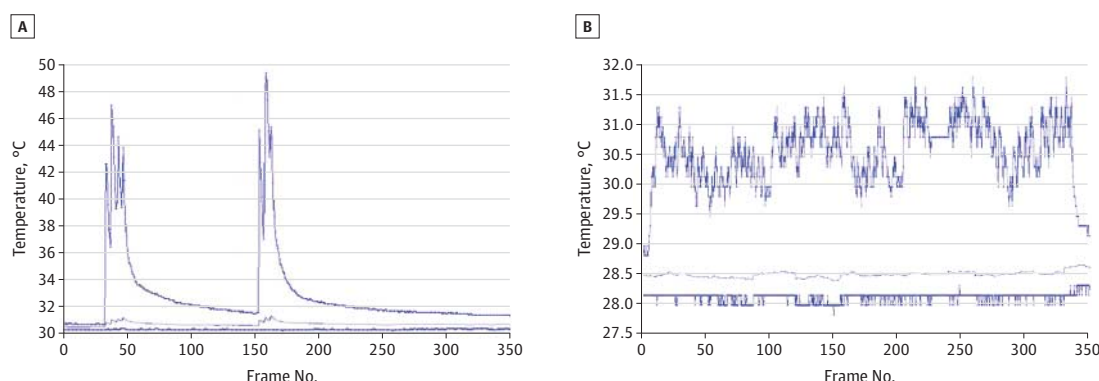
A, Thermogram for erbium:YAG laser ablation. B, Thermogram for picosecond infrared laser ablation.

range of the color gradient is narrower for the PIRL, from 28°C (black-blue) to 30°C (violet-white). The Er:YAG laser output beam (diameter of approximately 1 mm) is much larger than the PIRL (diameter, 300 μm); as such, it is programmed to ablate in a larger stepwise overlapping fashion than is the PIRL. On thermal imaging, this is seen as multiple distinct circular zones of approximately 1 mm in diameter (Figure 2A). The PIRL is programmed to ablate with much smaller continuous steps, and thus shows a more linear pattern on thermal imaging (Figure 2B).

The IRBIS 3plus software generates 3 data points for each frame captured, at a rate of 1 frame every 10 milliseconds. These 3 data points are the peak, minimum, and mean temperature within the capture area contained by the white circle seen on the thermal images in Figure 2. These data points are then used to plot thermographs, line graphs of the peak, minimum, and average temperatures (y-axis) for 10-millisecond time intervals (x-axis). **Figure 3** shows thermographs of pulsed ablation for the Er:YAG laser and PIRL. As would be expected for pulsed lasers, picket fence–like peaks are demonstrated. The highest line of peaks represents the maximum temperature, the middle line the mean temperature within the entire capture field, and the lowest line the baseline skin surface temperature (essentially the room temperature for the ex vivo skin used). The baseline skin surface temperature was 30.2°C during Er:YAG laser ablation and 28.1°C during PIRL ablation. The warm baseline temperatures were the result overhead lighting combined with warm ambient room temperatures; experiments were conducted in 2 separate rooms because the laser systems could not be easily transported. Because scanning patterns differ for Er:YAG laser and PIRL, different picket fence–like patterns are seen. In a 2-line pass, the Er:YAG laser thermogram shows 2 separate groupings of temperature peaks (Figure 3A). The PIRL ablates in a continuous fashion (Figure 3B). Despite the continuous pulsed nature of the PIRL ablation, heat generation during ablation remains significantly lower than during Er:YAG laser ablation.

The mean peak rise in skin surface temperature for the Er:YAG laser and PIRL was calculated at 15.0°C and 1.68°C, respectively ($P < .001$). Maximum peak rise in skin surface tem-

perature was 18.85°C for the Er:YAG laser and 2.05°C for the PIRL. Ablation craters were confirmed on digital microscopy.

Discussion

Real-time heat generation during Er:YAG laser ablation of ex vivo porcine skin, as measured by thermography, is significantly more than during PIRL ablation. At an Er:YAG laser ablation fluence of 2 J/cm² (just above the threshold fluence necessary for ablation to occur of 1.5 J/cm² for the Er:YAG laser), a mean temperature rise of 15°C and peak of 19°C was demonstrated. As discussed, irreversible thermal denaturation of human proteins may occur following short exposures to temperatures as low as 18°C above body temperature in the absence of thermal necrosis.[14-17] Thus cellular injury may result despite this low Er:YAG laser fluence. Furthermore, such changes on a molecular level would not be immediately evident on standard histologic analysis. As such, measuring real-time heat generation during laser ablation is an important adjunctive outcome measure. In clinical practice, much higher fluence levels are typically used, resulting in even higher peak temperatures.[11-13,19,20]

The PIRL allows photon energy to be deposited in a much more efficient fashion, driving photomechanical ablation with near complete thermal confinement. As a result, the PIRL ablates at a much lower fluence than the Er:YAG laser. Only clinically negligible mean and peak temperature rises of 2°C were seen during active PIRL ablation using a fluence level sufficient for ablation by the PIRL of 0.6 J/cm².

Study Limitations
This study is limited in that thermal characteristics of ex vivo skin differ from that of in vivo skin. A complex interplay of capillary blood flow and metabolic heat generation within in situ skin is responsible for maintaining temperature homeostasis. In addition, the water content and cellular integrity of ex vivo and in vivo skin differ considerably depending on time of harvest and preservation methods. To minimize these potential differences, skin samples used in this study were harvested fresh from an abattoir, refrigerated, and used within hours.

In addition, the thermography camera used in this study had a frame capture rate limited to 100 Hz; frames are captured in 10-millisecond intervals. There will be some thermal diffusion during this time that will reduce the maximum temperature recorded in this sampling time. Despite this measurement limitation, there is a clear reduction in the excessive heat deposited adjacent to the ablated tissue zone with the PIRL system compared with the Er:YAG laser. Improvements in the time resolution of the thermal imaging would nevertheless be of important value in correlating tissue damage and healing outcomes to the precise degree and duration of temperature elevations on adjacent tissue.

Future Studies

It is interesting to note that use of the Er:YAG laser at a fluence just less than 4 times that used for the PIRL resulted in a 9-fold increase in peak temperature rise. This effect is in part due to the enhanced efficiency of the PIRL system compared with the Er:YAG laser; lower fluence rates—and hence less total energy deposition—are required to ablate a given volume of tissue. However, even after differences in fluence rates are accounted for, the adjusted thermal rise is more than double for Er:YAG laser ablation compared with PIRL ablation. The explanation for this difference is found by comparing the ablation dynamics of the 2 systems. Compared with the Er:YAG laser, a far greater proportion of the PIRL's photon energy goes directly into powering the photomechanical ablation process, with a much lower proportionate loss due to energy spread outside the target area. The timescale is relevant; PIRL driven ablation occurs on a 100-picosecond timescale. With all short-pulsed lasers, some degree of excitation of recoil and acoustic modes within the target volume tissue occurs. In the nanosecond range and longer, these excitations propagate outwards from the target area, causing additional heating and damage to the surrounding tissue as previously discussed. In the picosecond range and shorter, the excited recoil and acoustic modes have frequency components on the order of 100 GHz (the Fourier transform of the ablation dynamics). Acoustics in this frequency range are strongly absorbed and hence do not propagate out of the ablation zone. The result is such that more energy is channeled into ablation instead of into heating of the surrounding tissue.[5,21] The picosecond time scale also completely avoids other effects typically seen with conventional short-pulse lasers, such as nucleation growth and cavitation-induced shock waves, further increasing the ablation drive efficiency. The differences in temperature measurements between the 2 laser systems presented herein are explained by these differences in their ablation dynamics.

The current PIRL setup is limited to a fluence of 0.6 J/cm². Soon, more powerful PIRL systems will be available, with improved cutting speeds and tissue ablation rates. Similar experiments using these higher fluence levels will be required, since the dynamics of heat transport and acoustic propagation out of the ablation zone are nonlinear; this characterization will be essential to ensure that PIRL scalpels are used at levels that retain negligible energy spread to adjacent tissue. Furthermore, standardization of ablation volumes will be necessary in future experiments to more precisely compare volume rates of ablation between laser systems.

In theory, photomechanical cold ablation should also be possible for osseous tissue using the PIRL, including cortical bone. Measurement of heat generation during PIRL ablation of osseous tissue is required as proof. In addition to in vivo soft-tissue experiments to measure heat generation, more research is needed on longitudinal healing studies for both soft and osseous tissues.

Conclusions

This experiment has demonstrated that PIRL photomechanical ablation is a more efficient process than Er:YAG laser–driven ablation. Furthermore, it has demonstrated that at fluence levels just above ablation threshold, temperature rises are negligible for PIRL ablation and significantly higher for Er:YAG laser–driven ablation. The negligible heat generation as measured for PIRL ablation confirms the potential of this novel technology in minimizing undesirable thermal injury associated with lasers currently in clinical use. This study provides evidence for genuine cold ablation of soft tissue using a non-ionizing ultrafast PIRL system.

Author Contributions: Dr Jowett had full access to all the data in the study and takes responsibility for the integrity of the data and the accuracy of the data analysis.
Study concept and design: Jowett, Wöllmer, Mlynarek, Wiseman, Franjic, Böttcher, Knecht, Miller.
Acquisition of data: Jowett, Wöllmer, Krötz.
Analysis and interpretation of data: Jowett, Segal, Miller.
Drafting of the manuscript: Jowett, Miller.
Critical revision of the manuscript for important intellectual content: All authors.
Statistical analysis: Jowett, Böttcher.
Obtained funding: Jowett, Wiseman, Knecht, Miller.
Administrative, technical, and material support: Wöllmer, Krötz, Böttcher.
Study supervision: Wöllmer, Mlynarek, Wiseman, Knecht, Miller.

REFERENCES

1. Loh SA, Carlson GA, Chang EI, Huang E, Palanker D, Gurtner GC. Comparative healing of surgical incisions created by the PEAK PlasmaBlade, conventional electrosurgery, and a scalpel. *Plast Reconstr Surg*. 2009;124(6):1849-1859.

2. Amini-Nik S, Kraemer D, Cowan ML, et al. Ultrafast mid-IR laser scalpel: protein signals of the fundamental limits to minimally invasive surgery. *PLoS One*. 2010;5(9):e13053.

3. Mahvash M, Voo LM, Kim D, Jeung K, Wainer J, Okamura AM. Modeling the forces of cutting with scissors. *IEEE Trans Biomed Eng*. 2008;55(3):848-856.

4. Vogel A, Venugopalan V. Mechanisms of pulsed laser ablation of biological tissues. *Chem Rev*. 2003;103(2):577-644.

5. Franjic K, Cowan ML, Kraemer D, Miller RJ. Laser selective cutting of biological tissues by impulsive heat deposition through ultrafast vibrational excitations. *Opt Express*. 2009;17(25):22937-22959.

6. Abu-Serriah M, Critchlow H, Whitters CJ, Ayoub A. Removal of partially erupted third molars using an Erbium (Er):YAG laser: a randomised controlled clinical trial. *Br J Oral Maxillofac Surg*. 2004;42(3):203-208.

7. Paltauf G, Dyer PE. Photomechanical processes and effects in ablation. *Chem Rev*. 2003;103(2):487-518.

8. Choi B, Barton JK, Chan EK, Welch AJ. Imaging of the irradiation of skin with a clinical CO_2 laser system: implications for laser skin resurfacing. *Lasers Surg Med*. 1998;23(4):185-193.

9. Pan TL, Wang PW, Lee WR, et al. Systematic evaluations of skin damage irradiated by an erbium:YAG laser: histopathologic analysis, proteomic profiles, and cellular response. *J Dermatol Sci*. 2010;58(1):8-18.

10. Martins GL, Puricelli E, Baraldi CE, Ponzoni D. Bone healing after bur and Er:YAG laser ostectomies. *J Oral Maxillofac Surg*. 2011;69(4):1214-1220.

11. Walsh JT Jr, Flotte TJ, Deutsch TF. Er:YAG laser ablation of tissue: effect of pulse duration and tissue type on thermal damage. *Lasers Surg Med*. 1989;9(4):314-326.

12. Alster TS, Lupton JR. Erbium:YAG cutaneous laser resurfacing. *Dermatol Clin*. 2001;19(3):453-466.

13. Weinstein C. Erbium laser resurfacing: current concepts. *Plast Reconstr Surg*. 1999;103(2):602-618.

14. Walsh JT Jr, Flotte TJ, Anderson RR, Deutsch TF. Pulsed CO_2 laser tissue ablation: effect of tissue type and pulse duration on thermal damage. *Lasers Surg Med*. 1988;8(2):108-118.

15. Gao YS, Su JT, Yan YB. Sequential events in the irreversible thermal denaturation of human brain-type creatine kinase by spectroscopic methods. *Int J Mol Sci*. 2010;11(7):2584-2596.

16. Dekhtyar Y, Gamza A, Tatarinov A, Jansons H. Electron and mechanical properties of bone during heating, evaluated by exoelectron emission and ultrasound. *Biomaterials*. 1995;16(11):861-863.

17. Arnoczky SP, Aksan A. Thermal modification of connective tissues: basic science considerations and clinical implications. *J Am Acad Orthop Surg*. 2000;8(5):305-313.

18. Campbell EM; Society of Photo-optical Instrumentation Engineers. *Femtosecond and Nanosecond High-Intensity Lasers and Applications: 17-18 January 1990, Los Angeles, California*. Bellingham, WA: SPIE; 1990.

19. Riggs K, Keller M, Humphreys TR. Ablative laser resurfacing: high-energy pulsed carbon dioxide and erbium:yttrium-aluminum-garnet. *Clin Dermatol*. 2007;25(5):462-473.

20. Stuzin JM, Baker TJ, Baker TM. CO_2 and erbium:YAG laser resurfacing: current status and personal perspective. *Plast Reconstr Surg*. 1999;103(2):588-591.

21. Franjic K, Miller D. Vibrationally excited ultrafast thermodynamic phase transitions at the water/air interface. *Phys Chem Chem Phys*. 2010;12(20):5225-5239.